

Thermal Motion - Evaluating Methods for Finding the Boltzmann Constant

Written By: Kelly Hong, Rayan Ramadan

Abstract

This investigation applied well studied methods for determining Boltzmann's constant k_B by analyzing the Brownian motion of micron-sized spheres in water. Three methods were used: Einstein's relation for mean squared displacement, curve fitting the Rayleigh distribution, and the maximum-likelihood estimation [1]. Each method was used to calculate the diffusion coefficient D . The Stokes Einstein relation [2] was then used to calculate Boltzmann's constant, k_B . Einstein's relation resulted in $k_B = (0.90 \pm 0.32) \times 10^{-23}$ [J/K], with the greatest percent error of 27%. Using Rayleigh's distribution resulted in $k_B = (1.02 \pm 0.13) \times 10^{-23}$ [J/K]. The maximum likelihood estimate resulted in $k_B = (1.07 \pm 0.14) \times 10^{-23}$ [J/K], providing the closest approximation relative to the accepted literature value of $k_B = 1.38 \times 10^{-23}$ [J/K] at a percent error of 22%. The value of k_B was consistently underestimated through these three methods, suggesting systematic errors in particle tracking or motion unaccounted for in the third spatial dimension, depth.

1. Introduction

The objective of this experiment is to determine Boltzmann's constant using Brownian motion and subsequently calculate Avogadro's number. Using molecular-kinetic theory, Einstein demonstrated that the mean-squared displacement of a Brownian particle increases linearly with time, resulting in Einstein's relation (1).

$$\langle x^2 \rangle = 2Dt \quad \text{where} \quad D = \frac{kT}{\gamma} \quad (1)$$

In the above relation (1) k_B is the Boltzmann's constant, D is the diffusion coefficient, η is the water viscosity, and r is the particle radius. Alternatively, the probability distribution for the distance travelled over a time interval can be used to calculate the Boltzmann's constant:

$$P(x, t) = \frac{1}{(4\pi Dt)^{\frac{1}{2}}} e^{-\frac{x^2}{4Dt}}. \quad (2)$$

However, since the experiment will be done on a 2-dimensional surface, the probability density function in a 2-dimensional diffusion process is therefore,

$$P(r; t) = \frac{r}{2Dt} e^{-\frac{r^2}{4Dt}}, \quad (3)$$

where t is the 'step' size (*not total time*) and r is the distance moved in 1 'step' (*not total distance*). This is also known as the Rayleigh distribution.

To address limitations of the least-squares method in the Python curve-fitting function, maximum likelihood estimation is used for the Rayleigh distribution:

$$(2Dt)_{est} = \frac{1}{2N} \sum_{i=1}^N r_i^2. \quad (4)$$

Finally, the Avogadro's number can be calculated using the Boltzmann's constant,

$$N_A = \frac{R}{k}, \quad (5)$$

where R is the gas constant.

2. Materials and Methods

The following section details materials, sample preparation, and data collection protocol, for the observation of the motion of micron-sized spheres in water.

2.1 Materials

The materials used in this experiment are presented visually below, including prepared sample slides and microscope settings.

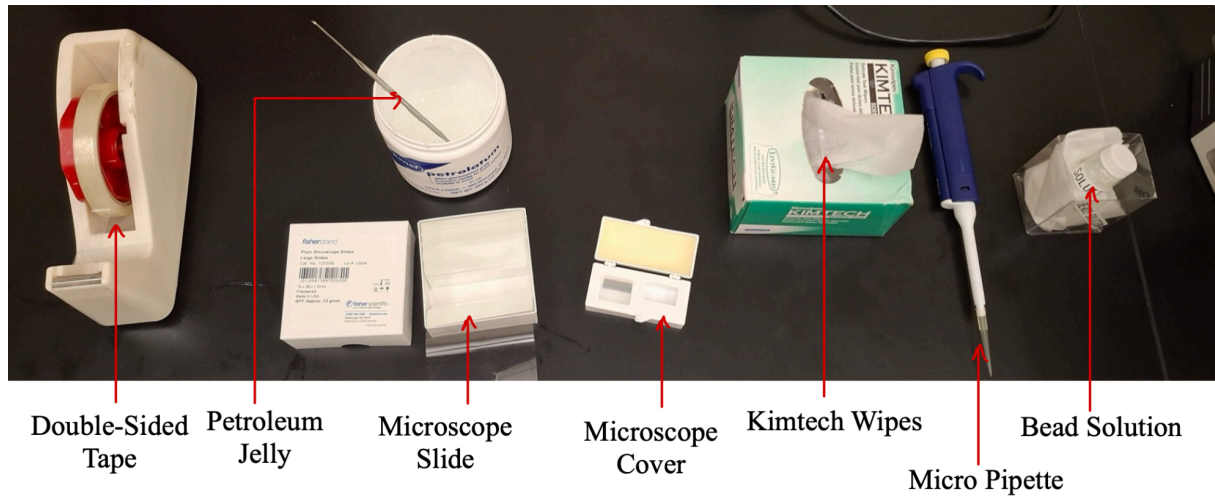


Figure 1: List of materials used for sample preparation.

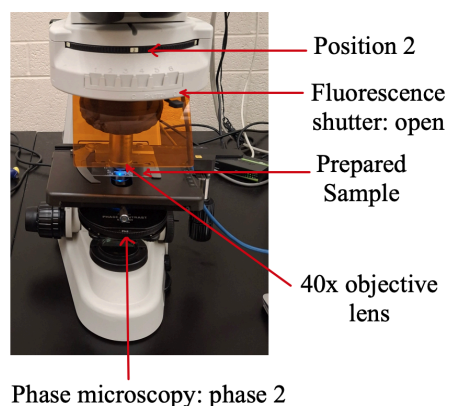


Figure 2: Microscope Set-up.

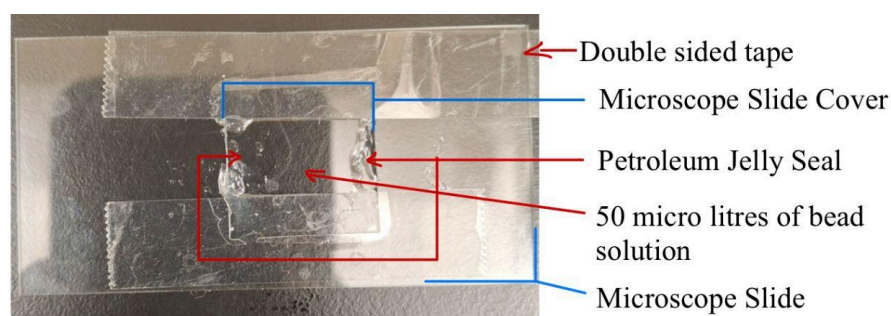


Figure 3: Prepared Sample Set-up

2.2 Procedure

We prepared 1 sample of 50 microliters of bead solution on a microscope slide as detailed in Fig. 1. The microscope was set to phase 1. Fluorescence illumination was switched on through the X-Cite box, the fluorescence cube was set in position 2 on the dial as indicated at the top of Fig 2: Microscope Set-up. The fluorescence shutter was set to open, and the prepared sample was placed on the microscope stage. Phase microscopy (Ph2, bottom dial in Fig. 2) was switched on, and the 40 x objective lens was used. Focusing the image to approximately the center of the preparation depth took time and continual small adjustments through the coarse and fine focus knobs.

The LabView application was run on the laboratory computer, and the microscope camera controller was turned on. The camera imaging setting on the microscope was turned on by pushing the lever in on the top right of the microscope. Gain and brightness values were adjusted to reach peak contrast between the beads (grey/white) and the background (black). Blurred bead boundaries led to poor tracking in the first few attempts, so contrast was increased and the image sharpened by adjusting the camera gain and brightness settings.

A plane with a few energized (moving) beads was located, and multiple image capture was set up to capture 120 frames at 2 frames per second. Once image capture of the 120 frames was complete, the data was saved and opened in the Image Object Tracker software, where a bounding box was placed over each dot captured in the images, and pixel coordinates of each frame were recorded in a .txt file.

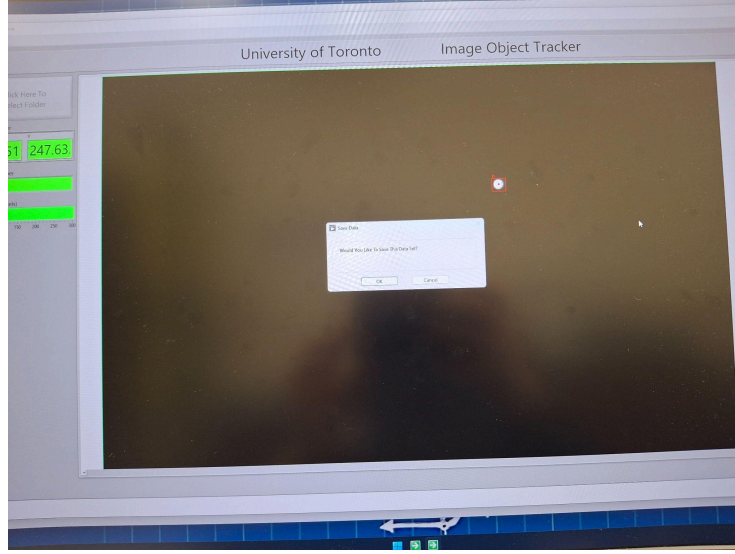


Figure 4: Image of bounding a visible bead using a tracking box on the Image Object Tracker software.

Once each bead was tracked in the set of frames, the microscope platform was shifted to capture a new set of beads on the sample slide, and the process was repeated a total of 12 times. Given an average of 3 beads were captured per cycle, this resulted in a total output of exactly 36 tracked beads.

3. Results and Analysis

In this section we detail 3 different methods for calculating k_B - using Einstein's relation, the Rayleigh distribution, and the maximum likelihood estimate (MLE).

3.1 Calculating Boltzmann Constant k_B Through Einstein's Relation

In this experiment, we determined the Boltzmann constant k_B using Einstein's relation for Brownian motion represented by Eq. (2). The diffusion coefficient D was determined from the slope of the mean-squared distance (MSD) vs. time plot for each particle (plot for one particle shown in Figure 5), using an alternative form of Eq. (1) for *2-dimensional* motion:

$$\langle x^2 \rangle + \langle y^2 \rangle = 4Dt, \quad (7)$$

where D and k_B can be calculated as follows:

$$D = \frac{\langle x^2 \rangle + \langle y^2 \rangle}{4t} = \frac{\text{slope}}{4} \Rightarrow k_B = \frac{6\pi\eta RD}{T} \quad (8)$$

We then calculated the Boltzmann constant k_B for the 36 tracked particles using Eq. (2), and compared each value to the accepted literature value for k_B , $k_B = 1.38 \times 10^{-23}$ [J/K] by calculating the percent error. These results are summarized below in Table 1.

Table 1. Percentage difference between calculator k -value and accepted k -value for each particle.

#	Calculated k_B [10^{-23} J/K]	Difference between accepted k_B [%]	#	Calculated k_B [10^{-23} J/K]	Difference between accepted k_B [%]
1	1.26 ± 0.11	8.7 ± 0.081	19	0.84 ± 0.07	39 ± 0.054
2	1.26 ± 0.11	8.7 ± 0.081	20	0.98 ± 0.87	29 ± 0.063
3	0.98 ± 0.87	29 ± 0.063	21	1.12 ± 0.10	19 ± 0.072
4	0.84 ± 0.07	39 ± 0.054	22	1.12 ± 0.10	19 ± 0.072
5	0.98 ± 0.87	29 ± 0.063	23	0.98 ± 0.87	29 ± 0.063
6	1.12 ± 0.10	19 ± 0.072	24	1.12 ± 0.10	19 ± 0.072
7	0.98 ± 0.87	29 ± 0.063	25	1.40 ± 0.12	1.4 ± 0.090
8	0.84 ± 0.07	39 ± 0.054	26	0.70 ± 0.06	49 ± 0.044
9	0.98 ± 0.87	29 ± 0.063	27	0.98 ± 0.87	29 ± 0.063
10	0.84 ± 0.07	39 ± 0.054	28	0.84 ± 0.07	39 ± 0.054
11	0.98 ± 0.87	29 ± 0.063	29	1.12 ± 0.10	19 ± 0.072
12	1.12 ± 0.10	19 ± 0.072	30	0.84 ± 0.07	39 ± 0.054
13	1.12 ± 0.10	19 ± 0.072	31	0.98 ± 0.87	29 ± 0.063
14	1.12 ± 0.10	19 ± 0.072	32	0.98 ± 0.87	29 ± 0.063
15	0.98 ± 0.87	29 ± 0.063	33	1.12 ± 0.10	19 ± 0.072
16	1.12 ± 0.10	19 ± 0.072	34	0.003 ± 0.0005	99 ± 0.00018
17	1.26 ± 0.11	8.7 ± 0.081	35	0.98 ± 0.87	29 ± 0.063
18	1.12 ± 0.10	19 ± 0.072	36	1.12 ± 0.10	19 ± 0.072

As shown above in Table 1, the results showed a wide range of percent errors between the calculated k and accepted k , varying from 1.4 ± 0.090 [%] to 99 ± 0.00018 [%]. The average uncertainties in this difference was 0.071 [%], reflecting the propagation of experimental uncertainties in D , γ , and T .

We include a sample of the cumulative squared distances travelled by the first four particles in a figure below, representative of the graphing and curve fitting process we adopted through Excel.

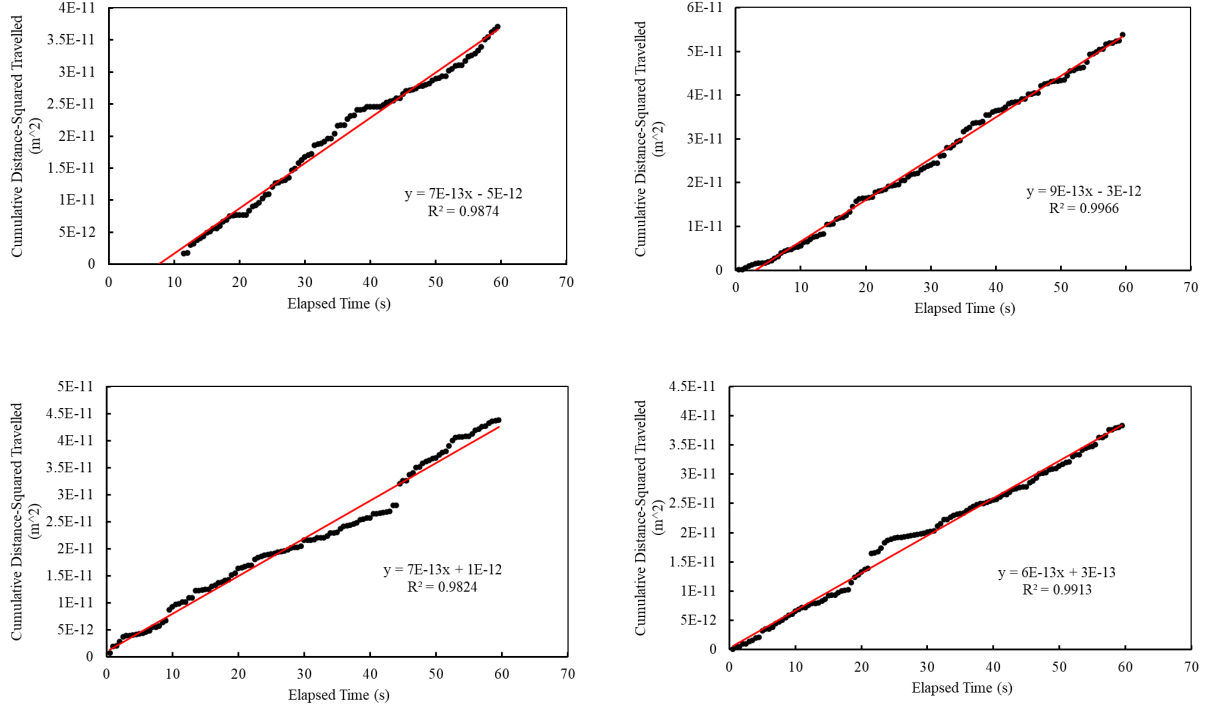


Figure 5. First 4 particles tracked and linearly curve fit in accordance with Einstein's relation.

We provide a sample calculation of k_B below for particle #2. The slope was found to be $m = 9 \times 10^{-13}$.

$$D = \frac{m}{4} = \frac{9 \times 10^{-13}}{4} = 2.25 \times 10^{-13}$$

$$\Rightarrow k_B = \frac{6\pi\eta RD}{T} = \frac{6\pi(0.933 \times 10^{-3})(0.95 \times 10^{-6})(2.25 \times 10^{-13})}{296.5} = 1.26 \pm 0.11 \text{ [J/K]}$$

Einstein's molecular-kinetic theory predicts that MSD increases linearly with time. This relationship is shown in Figure 5 above. However, as more time passes, the deviations from linearity increase. These deviations may result from the accumulation of tracking errors or limitations in the imaging system. Despite fitting the graph linearly in order to determine the diffusion coefficient D , the calculated values of the Boltzmann constant k_B vary significantly between different particles, with some deviating at a percent error as small as 1.4 ± 0.090 [%] and others as much as 99 ± 0.00018 [%] from the accepted value. The significant differences could be a result from the errors previously mentioned.

The uncertainty in k was calculated using propagation of errors from the diffusion coefficient D , friction coefficient γ , and temperature T , as shown in the following equation:

$$\frac{\Delta k}{k} = \sqrt{\left(\frac{\Delta D}{D}\right)^2 + \left(\frac{\Delta \gamma}{\gamma}\right)^2 + \left(\frac{\Delta T}{T}\right)^2}. \quad (9)$$

The uncertainty for the diffusion constant D was calculated using the linear fitter and uncertainties of parameters. The slope uncertainty s_m was calculated using the following equation:

$$s_m = \sqrt{\frac{s_{y(x)}^2}{N\Delta^2}}, \quad (10)$$

where

$$s_{y(x)}^2 = \frac{1}{N-2} \sum (y_i - (b + mx_i))^2, \quad (11)$$

And

$$\Delta = N \sum x_i^2 - (\sum x_i)^2. \quad (12)$$

Since $D = \frac{m}{4}$, the uncertainty s_d in D is propagated from the uncertainty in the slope: $s_d = \frac{s_m}{4}$.

Thus, the diffusion coefficient with uncertainty is:

$$D \pm s_D = \frac{slope \pm s_m}{4}. \quad (13)$$

The resulting uncertainties for the calculated Boltzmann constant and the difference between it and the accepted value provides a quantitative measure of error. Although all uncertainties were propagated, the wide range of percent differences between the calculated and accepted value of k suggests the presence of systematic sources of error rather than random fluctuations. This highlights the need for further discussion regarding the sources of error and improvements in tracking methodology. A more detailed discussion of these errors and their potential impact on the results follows in section 4.1 below.

After calculating all the values and uncertainties, we found the average of all values found using Einstein's relation to yield $k_B = (0.90 \pm 0.32) \times 10^{-23}$ [J/K].

The R^2 values of all the graphs regarding the motion of the 36 particles ranged from 0.482 to 0.998, with the average of all values being 0.966. Since this value is very close to 1, this is a very strong fit, suggesting that the model generally describes the motion of the particles very well.

3.2 Calculating the Boltzmann Constant k_B using the Rayleigh distribution

All distances travelled within a 0.5 second time interval were included in a 1-dimensional array, forming an array containing a total of 119×36 , or $n = 4284$, data points. These distances were placed in a histogram distribution with a bin size “b” optimally selected using the Freedman Diaconis rule for skewed distributions [3].

$$b = 2 \frac{IQR(r)}{(n^{1/3})} = 2 \frac{4.01 \times 10^{-7}}{(4284^{1/3})} = 4.94 \times 10^{-8} m \quad (14)$$

The formula above was used to calculate the bin width b, where the IQR is the interquartile range, or the range of distances traveled falling between the 25% most frequent distances travelled and 75% most frequent distances travelled by the particles, and where n is the number of data points (n=4284).

Here we plot the 4284 data points on a histogram with bins of width b spanning the minimum and maximum step sizes. While the bin width would be sensitive to outliers given a set number of bins, this is accounted for using the Freedman Diaconis estimation through the inclusion of the IQR. The histogram is fit to a Rayleigh distribution using sci-py’s curve_fit function.

$$p(r; t = 0.5) = \frac{r}{2Dt} e^{-\frac{r^2}{4Dt}} = \frac{r}{D} e^{-\frac{r^2}{2D}} \quad (15)$$

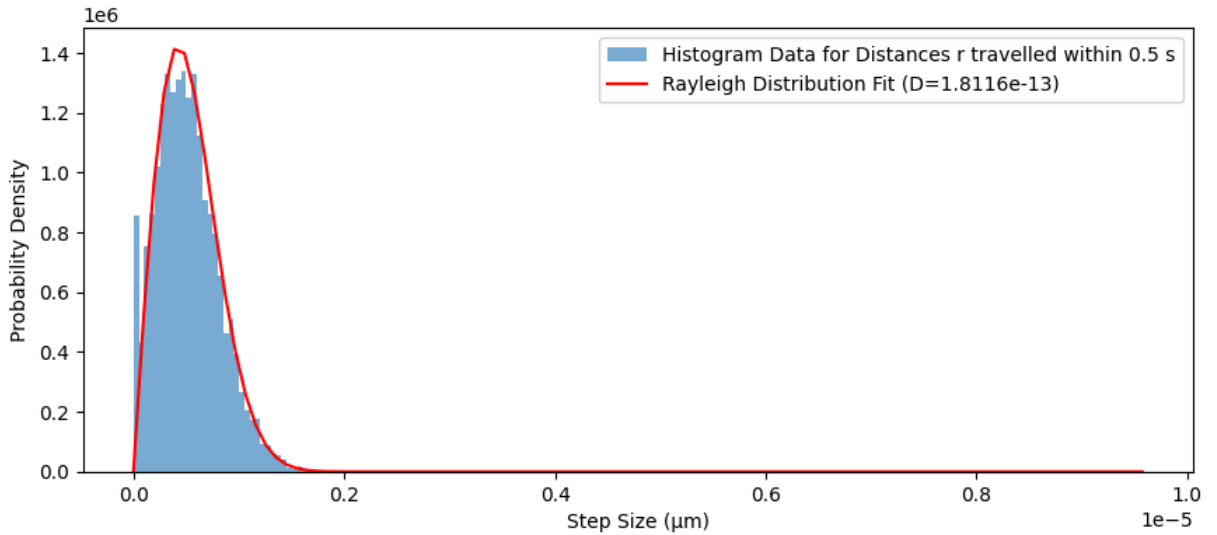


Figure 6: Distribution of distances (μm) travelled by individual particles in 0.5 s time intervals curve fit to a Rayleigh distribution.

The fit parameters were extracted, and the diffusion coefficient D was returned by the above curve fit using SciPy's `curve_fit` function to be $D = 1.81 \times 10^{-13} \text{ m}^2/\text{s}$. k_B was calculated using the Einstein Stokes relation below [2].

$$D = \frac{kT}{\gamma} \Rightarrow k_B = \frac{\gamma D}{T}, T = 296.5 \text{ K}, \gamma = 6\pi\eta r, \text{ and radius } R = 0.95 \pm 0.1 \mu\text{m}.$$

$$k_B = \frac{6\pi\eta R D}{T} = \frac{6\pi(0.933 \times 10^{-3}) (0.95 \times 10^{-6}) (1.81 \times 10^{-13})}{296.5} = (1.02 \pm 0.13) \times 10^{-23} \text{ J/K}$$

The above calculation demonstrates a 26.03% percent error from the accepted value of k .

The uncertainty for k_B was estimated using the standard deviation of the distribution. The variance of the distribution was extracted using SciPy, and used to approximate the uncertainty on the fit parameter D as shown below.

$$\sigma_D = \sqrt{\text{Var}(D)} = \sqrt{1.2 \times 10^{-29}} = \pm 3.5 \times 10^{-15}$$

$$\Delta k_B = \sqrt{\left(\frac{6\pi R D}{T} \Delta \eta\right)^2 + \left(\frac{6\pi \eta D}{T} \Delta R\right)^2 + \left(\frac{6\pi \eta R}{T} \sigma_D\right)^2 + \left(-\frac{6\pi \eta R D}{T^2} \Delta T\right)^2} = \pm 0.13 \times 10^{-23} \text{ J/K}$$

The variance of the fit was 1.2×10^{-29} . This extremely low variance suggests an over-fitted model. This is expected for the already established relationship between the probability distribution of particle movement and the Rayleigh distribution (15). Analogously, this same diffusion process in three dimensions could be perfectly curve-fit with the Maxwell-Boltzmann distribution [1].

3.3 Calculating the Boltzmann Constant k_B using the Maximum-Likelihood Estimate (MLE).

The curve-fitting method used in section 3.2 to calculate k_B was especially sensitive to bin size. To validate our results in section 3.2, we provide an additional calculation of k_B using the maximum-likelihood estimate (MLE). The formula for the MLE of a Rayleigh distribution is provided below.

$$(2Dt)_{est} = \frac{1}{2N} \sum_{i=1}^N r_i^2 \quad (16)$$

where r_i is each individual distance travelled, t the time interval, and N the number of data points. The list of distances travelled was compiled into a 1-D array of $N = 4284$ data points.

$$(D)_{est} = \frac{1}{2(4284)} (1.63 \times 10^{-9}) = (1.9 \pm 0.12) \times 10^{-13}$$

Following a process identical to section 3.2, we calculate k_B below.

$$k_B = \frac{6\pi\eta RD}{T} = \frac{6\pi(0.933 \times 10^{-3})(0.95 \times 10^{-6})(1.9 \times 10^{-13})}{296.5} = (1.069 \pm 0.14) \times 10^{-23} J/K$$

With the following percent error E_p :

$$E_p = \frac{k_b - (k_b)_{est}}{k_b} = \frac{(1.38 \times 10^{-23}) - (1.07 \times 10^{-23})}{1.38 \times 10^{-23}} = 0.22 \Rightarrow 22\% \text{ error}$$

We calculate the uncertainty on D and k_B shown above using the following set of formulae for error propagation.

$$D_{est} = \frac{1}{4tN} \sum_{i=1}^N r_i^2 \Rightarrow (\Delta D)^2 = \left(\frac{\partial D}{\partial t} \Delta t\right)^2 + \left(\frac{\partial D}{\partial S} \Delta S\right)^2 \text{ where } S = \sum_{i=1}^N r_i^2$$

$$\frac{\partial D}{\partial t} = -\frac{1}{4t^2 N} \sum_{i=1}^N r_i^2 \text{ and } \frac{\partial D}{\partial S} = \frac{1}{4tN} \Rightarrow \Delta D = \frac{1}{4tN} \sqrt{\left(\frac{\Delta t}{t}\right)^2 + (\Delta S)^2}$$

The uncertainty in time, Δt , is given to equal ± 0.03 s. The uncertainty in S is calculated below.

We denote the uncertainty in S as σ_S .

$$S = \sum_{i=1}^N r_i^2$$

$$\Delta r_i^2 = \frac{\partial r_i^2}{\partial r_i} \Delta r_i = 2r_i \Delta r_i$$

$$\Delta S = \Delta \left(\sum_{i=1}^N r_i^2 \right) = \sqrt{\sum_{i=1}^N (2r_i \Delta r_i)^2}, \text{ where } \Delta r_i \text{ is claimed to be a value greater than } 0.1 \mu m [1].$$

For the purposes of this report, we use the value of $0.1 \mu m$ provided by the lab manual [1], and multiply it by $\sqrt{2}$, to account for errors in both the x and y directions.

Following this approximation, we use excel to calculate $\Delta S = 1.14 \times 10^{-11} m$. Using the above derivation for the uncertainty on D , we have the following.

$$\Delta D = \frac{1}{4tN} \sqrt{\left(\frac{\Delta t}{t} \sum_{i=1}^N r_i^2\right)^2 + (\Delta S)^2} = \frac{1}{4(0.5)(4284)} \sqrt{\left(\frac{0.03}{0.5} \times (1.6 \times 10^{-9})\right)^2 + (1.1 \times 10^{-11})^2}$$

$$\Delta D = \pm 1.2 \times 10^{-14}$$

Given we calculated k_B using the following equation, we further propagate error to calculate Δk_B .

$$k_B = \frac{6\pi\eta RD}{T} \Rightarrow \Delta k_B = \sqrt{\left(\frac{\partial k_B}{\partial \eta} \Delta \eta\right)^2 + \left(\frac{\partial k_B}{\partial R} \Delta R\right)^2 + \left(\frac{\partial k_B}{\partial D} \Delta D\right)^2 + \left(\frac{\partial k_B}{\partial T} \Delta T\right)^2}$$

$$\Delta k_B = \sqrt{\left(\frac{6\pi RD}{T} \Delta \eta\right)^2 + \left(\frac{6\pi \eta D}{T} \Delta R\right)^2 + \left(\frac{6\pi \eta R}{T} \Delta D\right)^2 + \left(-\frac{6\pi \eta RD}{T^2} \Delta T\right)^2}$$

$$\Delta k_B = \pm 1.4 \times 10^{-24}$$

These values reflect an approximately 13% uncertainty, which is consistent with what was approximated as the uncertainty in the distances measured (10%). This implies that the greatest source of uncertainty was in the distance measurements, as they were summed over N=4284 values.

3.4 Summary of k_B values calculated using Einstein's relation, the Rayleigh Distribution, and the Maximum-Likelihood Estimate (MLE).

Here we summarize the results of the three methods used to calculate the Boltzmann constant k_B : (a) Einstein's relation, (b) curve-fitting the Rayleigh distribution, and (c) the maximum-likelihood estimate, in a single table.

Table 2. Comparison between 3 different methods of calculating k_B .

3.1. Einstein's Relation		3.2. Rayleigh Distribution (Curve-Fit)		3.3. Maximum-Likelihood Estimate (MLE)	
$k_B (\times 10^{-23} \text{ J/K})$	Percent Error (E_p)	$k_B (\times 10^{-23} \text{ J/K})$	Percent Error (E_p)	$k_B (\times 10^{-23} \text{ J/K})$	Percent Error (E_p)
0.90 ± 0.32	27%	1.02 ± 0.13	26%	1.07 ± 0.14	22%

4. Discussion

In this section, we compare the values of the Boltzmann constant k_B derived from each method, and discuss possible errors that may have affected our experimental results.

4.1 Comparison of Results from Sections 3.1 to 3.3

The notable differences in the k_B values calculated between the three methods reflects assumptions made in each of the methods. For example, curve-fitting the Rayleigh distribution to the distance travelled distribution of the particles violated key assumptions of the least-squares fitting process. Our selection of the bin-size for the distance travelled results in an inherent dependence between different bins as we can, for example, arbitrarily split up the frequency of steps in bin n between bin $n - \frac{1}{2}$ and $n + \frac{1}{2}$. The error and variance would then depend on the bin count as well as the actual data collected. This can result in overfitting the data. This is why we a) selected the bin size using the Freedman Diaconis estimation and b) validated our results in 3.2 with the maximum-likelihood estimate in 3.3.

Interestingly, all three k_B values calculated in the methods from 3.1 to 3.3 fell within 0.17×10^{-23} [J/K] of each other, however their mean fell 0.38×10^{-23} [J/K] away from the accepted literature value for k_B . This is highly indicative of a systematic error that under predicts k_B . An underpredicted k_B likely suggests that we are under-estimating the mean squared distance travelled. It is possible that this is due to restricting our measurements to two dimensions. Some of the energy of each particle might be going towards motion in the z-axis direction (depth). The fact that our temperature measurement goes towards 3 dimensional motion, while we only measure motion in two dimensions, indicates that we may be underestimating the total motion of the particle as we are not bounding each particle to a single z value or depth of vision. Underestimating r results in underestimating the diffusion coefficient D , which then can result in underestimating k_B as we have done throughout our analysis.

Our calculations resulted in low uncertainties due to the fairly precise nature of our experimental set-up. Using a microscope and a tracker software meant that we were able to track the motion of microscopic objects within fractions of a second. Increasing the contrast and sharpness of the images meant that our object tracking software was able to be very precise, though we had to remove many outlier measurements due to glitches in the software. This all suggests very low experimental uncertainty and random error, while our above discussion suggests high systematic error. Additional sources of error are discussed below.

4.2 Additional Sources of Errors

Even though our experimentally calculated values of the Boltzmann constant k varied significantly across the 36 trials, the general trend in every graph presents an agreement with

Einstein's theoretical prediction that the mean squared displacement increases linearly with time. This suggests that, despite errors in individual calculations of k_B , the underlying diffusion process was still well captured by our measurements.

The significant range of variation across our calculated k highlights the impact of systematic and random errors in the experiment. The following are possible errors that could have impacted our experimental results:

1. Inaccurate particle tracking: Some particles exhibited very large deviations (up to 99%) from the accepted k . There were data that showed large displacement jumps, which significantly affected the MSD slope, as shown in Figure 7. This is likely due to faulty image capturing or misidentifying bead positions while using the tracking software. To minimize the effect of this possible error and receive a more accurate line of best fit for calculating the MSD slope, these outliers were omitted (Figure 8). Higher-resolution imaging and more frequent calibration of the pixel-to-distance conversion factor could help minimize this error.

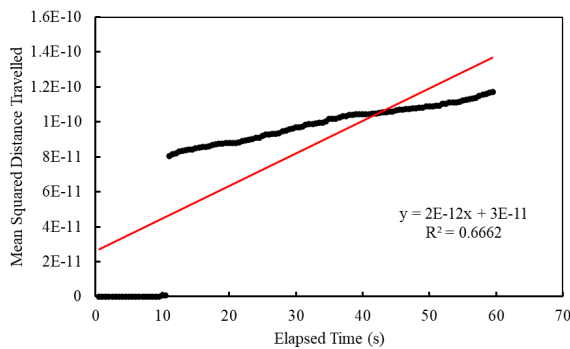


Figure 7. MSD plot for a particle, with data at the beginning showing no displacement, likely due to faulty tracking software.

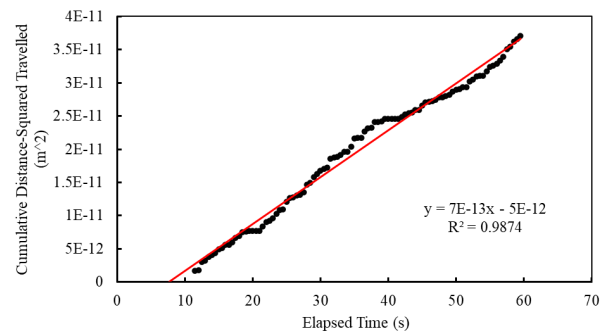


Figure 8. Same MSD plot as Figure 7, but with outliers omitted, resulting in a more accurate line of best fit.

2. Parallax Error from Microscope Focal Length and Depth of Vision: While we focused the image to the best of our abilities as per the methodology, it is possible that there was parallax error from not imaging the particles at the correct depth. The variation in k_B calculated for each particle's trajectory could be due to different particle depths on the microscope plate. The particle radius of $R = 0.95 \pm 0.1 \mu\text{m}$ could easily result in relatively large differences in particle depths relative to the focal plane of the images being taken. This could have resulted in the conversion factor between pixels and meters to only be accurate for a subset of the particles tracked, affecting Einstein's relation estimate process, the Rayleigh distribution curve fitting process, and the maximum-likelihood estimate as well. If most of these particles were farther than the depth

of vision, this would result in underestimates of the distances travelled, resulting in smaller slopes calculated for Einstein's relation and resulting in an underestimated k_B .

Variation in particle depth, and an inaccurately calibrated microscope depth could explain the consistently underestimated k_B values from all three processes. While the uncertainties calculated for all of them were insignificant, at around 15% uncertainty, the three values were a) very close to each other, presenting a range of 0.17×10^{-23} [J/K] between the highest and lowest k_B values. All three calculations underestimated the literature value for k_B suggesting a systematic error.

3. Temperature fluctuations: The viscosity η of water was adjusted for temperature, assuming a 2% decrease per °C. As the equation for calculating the friction coefficient γ is

$$\gamma = 6\pi\eta r,$$

where $r = (0.95 \pm 0.05) \times 10^{-6}$ [m] is the radius of a single bead, any errors in temperature measurement due to temperature fluctuations in the lab would directly affect η , influencing γ , and consequently affecting k .

Conclusion

The calculated Boltzmann constant k_B using Einstein's method, Rayleigh distribution, and maximum likelihood estimation are $k_B = (0.90 \pm 0.32) \times 10^{-23}$ [J/K] using Einstein's method, $k_B = (1.02 \pm 0.13) \times 10^{-23}$ [J/K] using the Rayleigh distribution, and $k_B = (1.07 \pm 0.14) \times 10^{-23}$ [J/K] using the maximum-likelihood estimate. The maximum-likelihood estimation yielded the closest approximation to the accepted value of $k_B = 1.38 \times 10^{-23}$ [J/K] with a 22% error, while the other methods showed slightly higher deviations. All methods were consistent with theoretical expectations, however, significant variations in calculated values likely resulted from errors such as tracking inaccuracies and temperature fluctuations. Standardizing conditions and calibrating depth of vision in future experiments can help reduce the systematic errors observed throughout this investigation.

References

[1] R. M. Serbanescu and W. Ryu, “Thermal Motion Revisions Introduction and Historical Facts,” 2008. Available: https://www.physics.utoronto.ca/~phy224_324/LabManuals/ThermalMotion.pdf.

[2] “The Stokes-Einstein Equation,” *NanoTemper Technologies*, 2024. Available: <https://support.nanotempertech.com/hc/en-us/articles/23851436308625-The-Stokes-Einstein-Equation>.

[3] Nkugwa Mark William, “How to Determine Bin Width for a Histogram (R and Python),” *Medium*, Oct. 31, 2023. Available: <https://nkugwamarkwilliam.medium.com/how-to-determine-bin-width-for-a-histogram-r-and-pyth-653598ab0d1c>.